行政院國家科學委員會專題研究計畫 期中進度報告

新穎金屬氧化物之研究--子計畫五：鎢系氧化物之超導,奈米結構,與其物理特性(2/3)
期中進度報告(精簡版)

計 畫 類 別 ：整合型
計 畫 編 號 ：NSC 94-2112-M-032-003-
執 行 期 間 ：94 年 08 月 01 日至 95 年 07 月 31 日
執 行 單 位 ：淡江大學物理學系

計 畫 主 持 人：錢凡之
共 同 主 持 人：林大欽

處 理 方 式 ：本計畫可公開查詢

中 華 民 國 96 年 12 月 06 日

Journal of Superconductivity and Novel Magnetism, Vol. 20, No. 3, April 2007 (© 2007)
DOI: 10.1007/s10948-006-0186-3

Effect of Oxygen Concentration on Superconducting Properties of Rubidium Tungsten Bronzes Rb_xWO_y

L. C. Ting,[1] H. H. Hsieh,[2] H. H. Kang,[1] D. C. Ling,[1] H. L. Liu,[3] W. F. Pong,[1] F. Z. Chien,[1] and P. H. Hor[4]

Received October 1, 2005; accepted November 16, 2005; Published online: 23 January 2007

Superconducting transition temperature (T_c) as a function of oxygen concentration for hexagonal rubidium tungsten bronzes Rb_xWO_y with $2.80 \leq y \leq 3.07$ and $x = 0.19$, 0.23, and 0.27 has been systematically investigated. Three regions corresponding to $T_c < 2\,K$ (denoted as superconductivity suppressed region), $T_c \sim 3\,K$ (superconductivity uniform region) and $T_c > 3\,K$ (superconductivity enhanced region) were identified in T_c–y phase diagram for $Rb_{0.19}WO_y$ and $Rb_{0.23}WO_y$. No superconductivity enhanced region was observed for $Rb_{0.27}WO_y$. The superconductivity suppressed region shifts toward higher oxygen content as rubidium concentration increases. The local ordering of the intercalated rubidium atoms might be responsible for the intriguing T_c–y phase diagram of Rb_xWO_y.

KEY WORDS: rubidium tungsten bronzes; oxygen concentration; superconductivity.

1. INTRODUCTION

The alkali tungsten bronzes were among the first oxides discovered to be superconducting [1]. The compounds, commonly referred as the tungsten bronzes, take a nonstoichiometric form of M_xWO_3 where M represents a metal atom and x ranges from near 0–1. These materials crystallize in various phases, namely tetragonal tungsten bronze (TTB), hexagonal tungsten bronze (HTB), and intergrowth tungsten bronze (ITB), depending on the size and valence of the metal ion M as well as its concentration x [2]. The corner-sharing WO_6 octahedra in these phases form 4-, 5-, and 6-membered rings, giving rise to tetragonal, pentagonal and hexagonal tunnels along the c-direction correspondingly. The radius of the tunnels is about 2.0 Å, which opens a channel to intercalate a wide variety of metallic ions with a comparable size. For example, the TTB phase of $Na_{0.3}WO_3$ and $Pb_{0.33}WO_3$ are found to have tetragonal and pentagonal tunnels, respectively [3]. The hexagonal tunnels are in the HTB phase of Rb_xWO_3 with $0.19 \leq x \leq 0.33$ [4]. The ITB phase of Sn_xWO_3 consists of single or double row of hexagonal tunnels intergrown between slabs of WO_3-like materials for $x = 0.04$ and 0.18, respectively [5].

This conclusion has been drawn on investigating the electronic and superconducting properties of the TTB Na_XWO_3 [6,7], which has an insulating parent compound of WO_3. NMR studies have shown that the electronic states in metallic Na_XWO_3 are similar to those in ReO_3 [8,9]. The sodium atoms only give out their s electrons to the conduction band whose bottom is built of W-$5d(t_{2g})$ orbitals hybridized with that of the O-$2p$ [10]. It was argued that the increase of superconducting transition temperature in Na_XWO_3 with decreasing sodium content is likely due to the poor screening of the electron-phonon interaction in the low sodium regime. However, it was pointed out by Brusetti *et al.* [11] that the screening mechanism is probably not very effective in the HTB phase of Rb_xWO_3, since the variation of T_c with

[1]Department of Physics, Tamkang University, Tamsui 251, Taiwan, ROC.
[2]Department of Applied Physics, Chung-Cheng Institute of Technology, Ta-Hsi 335, Taiwan, ROC.
[3]Department of Physics, National Taiwan Normal University, Taipei 116, Taiwan, ROC.
[4]Department of Physics, University of Houston, Houston, TX 77004, USA.

rubidium concentration x in the range of $0.23 \leq x \leq 0.28$ does not follow the commonly observed trend of increasing T_c with decreasing x [4]. Instead, it was suggested that the rubidium-ordering-induced structural instability of the lattice might be responsible for the anomalous $T_c(x)$ dependence [12–15].

In this paper, an alternative approach, by varying oxygen concentration in Rb_xWO_y, was taken to address the unsettled issue. We report the oxygen concentration dependence of the T_c for Rb_xWO_y with $x = 0.19, 0.23, 0.27$ and $2.80 \leq y \leq 3.07$. The key finding of this work is that the anomalous $T_c(x)$ dependence for Rb_xWO_3 with $0.23 \leq x \leq 0.28$ reported earlier is likely associated with a small deviation of the oxygen concentration from 3.00. In addition, another interesting finding is that there is no correlation between superconductivity and oxygen-concentration-dependent metal–nonmetal transition observed in Rb_xWO_y with $y \sim 3.00$.

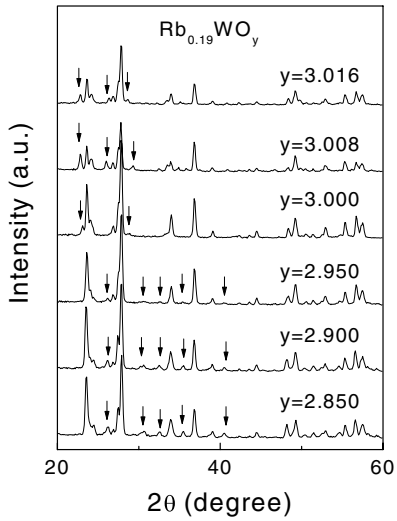

Fig. 1. X-ray diffraction patterns of $Rb_{0.19}WO_y$ with 2θ ranging from 20° to 60° for $2.850 \leq x \leq 3.016$. The impurity phases are marked by the arrows.

2. EXPERIMENTAL

Samples investigated were prepared by the solid-state reaction method. The proper stoichiometric amounts of high purity powders of Rb_2WO_4, WO_3, and W were thoroughly mixed and ground, then pressed into pellets. Subsequently, the pellets were sealed in quartz tubes in vacuum with pressure of 10^{-2} Torr. Samples were fired at 650°C for 5 h followed by heating at 850°C for 15 h. The X-ray measurements were carried out using Cuk_α radiation from Rigaku 12 kW RU200 X-ray generator. The resistivity measurements were made by a standard four-probe method. The magnetic properties of the samples were performed by Quantum Design SQUID magnetometer and PPMS.

3. RESULTS AND DISCUSSIONS

The X-ray diffraction (XRD) patterns of Rb_xWO_y with 2θ ranging from 20° to 60° for $2.80 \leq y \leq 3.07$ and $x = 0.19$, 0.23, and 0.27 are shown in Figs. 1–3. It should be mentioned that the rubidium concentration $x = 0.23$ and 0.27 were strategically chosen to be fallen in the region of $0.23 \leq x \leq 0.28$ with the unusual $T_c(x)$ dependence [4]. The XRD patterns clearly reveal that the predominant phase in the samples is hexagonal Rb_xWO_y with space group *P*63/*mcm* reported by Magneli [17]. As shown in Fig. 1, the impurity phase exists in $Rb_{0.19}WO_y$ samples throughout the entire range of the oxygen concentration investigated. The amount of impurity phase decreases with increasing oxygen concentration for all samples studied. The impurity free samples were synthesized in $Rb_{0.23}WO_y$ for $y \geq 2.97$ and in $Rb_{0.27}WO_y$ for $y \geq 3.00$ as illustrated in Figs. 2 and 3, respectively. It appears that the diffraction

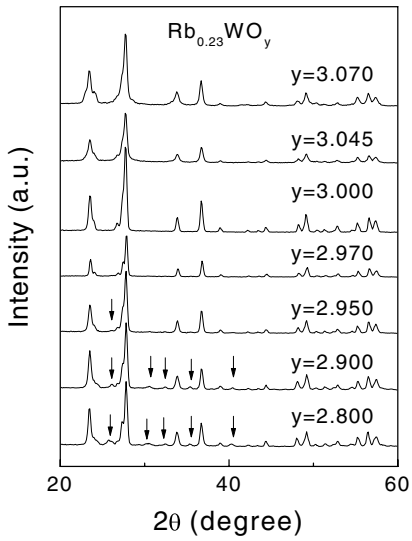

Fig. 2. X-ray diffraction patterns of $Rb_{0.23}WO_y$ with 2θ ranging from 20° to 60° for $2.800 \leq x \leq 3.070$. The impurity phases are marked by the arrows.

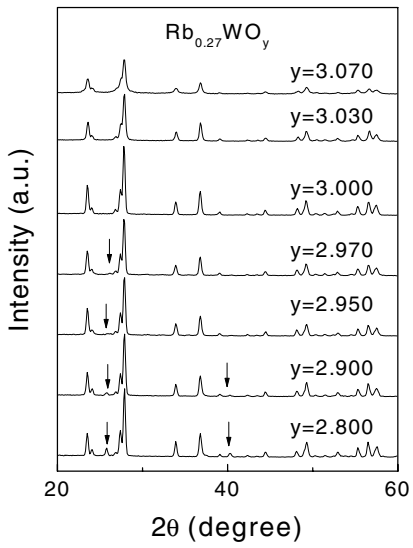

Fig. 3. X-ray diffraction patterns of $Rb_{0.27}WO_y$ with 2θ ranging from 20° to 60° for $2.800 \leq x \leq 3.070$. The impurity phases are marked by the arrows.

peaks broaden significantly as the oxygen concentration reaches 3.07, indicative of a poorly crystalline phase present.

The representative zero-field-cooled (ZFC) magnetic susceptibility curves for $Rb_{0.23}WO_y$ with $y = 2.82, 2.85, 3.03$, and 3.04 in a field of 10 G are displayed in Fig. 4(a). It should be noted that oxygen deficient samples with $y < 3.00$ have a lowerT_c around 3 K and a sharper superconducting transition width,

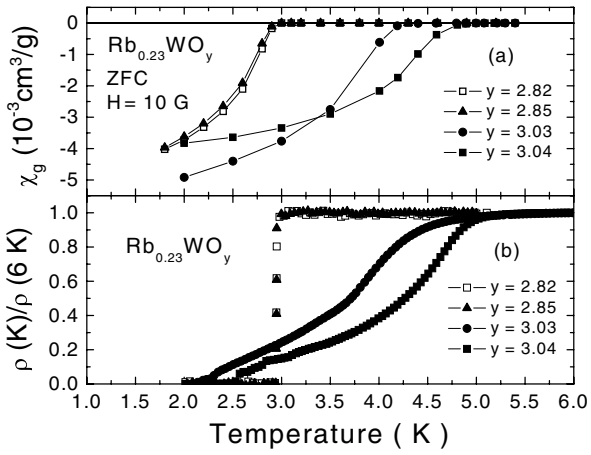

Fig. 4. (a) The ZFC magnetic susceptibility curves for $Rb_{0.23}WO_y$ with $y = 2.82, 2.85, 3.03$ and 3.04 in a field of 10 G. (b) Normalized resistivity as a function of temperature for for $Rb_{0.23}WO_y$ with $y = 2.82, 2.85, 3.03$ and 3.04.

whereas oxygen excess samples with $y > 3.00$ have a higher T_c around 5 K and a wider superconducting width. In addition, the measured dimensionless magnetic susceptibility χ around 2 K of both the oxygen excess samples and the oxygen deficient samples is about 0.02, which is approximately one quarter of $1/4\pi$, indicating that bulk superconductivity present in the $Rb_{0.23}WO_y$ with $y = 2.82, 2.85, 3.03$, and 3.04. The temperature dependence of the normalized resistivity for the sample mentioned above is displayed in Fig. 4(b). The superconducting transition temperature and the transition width obtained from resistivity measurements are remarkably in good agreement with those determined from magnetic measurements.

The temperature dependence of the resistivity for $Rb_{0.19}WO_y$ with $y = 3.00$ and 3.02, and for $Rb_{0.23}WO_y$ with $y = 2.85$ and 3.04 is illustrated in Fig. 5(a) and (b), respectively. As shown in the figure, normal-state resistivity of the samples with oxygen concentration $y > 3.00$ is about three orders of magnitude larger than that of those with oxygen concentration $y \leq 3.00$, regardless of the value of rubidium concentration x. In contrast to that, T_c of the samples is not as sensitive to the oxygen concentration y as the normal-state resistivity of the samples is. Furthermore, it is interesting to note that the metallic behavior observed in the normal-state of $Rb_{0.19}WO_{3.00}$ and $Rb_{0.23}WO_{2.85}$ is a common behavior for Rb_xWO_y samples with lower oxygen contents ($y \leq 3.00$), while the semiconducting-like feature observed in the normal-state of $Rb_{0.19}WO_{3.02}$ and $Rb_{0.23}WO_{3.04}$ is a general trend for Rb_xWO_y samples with higher oxygen concentrations ($y > 3.00$). The observed results indicate that the normal-state transport properties are not intimately related with superconductivity in Rb_xWO_y.

Figure 6 shows superconducting transition temperature as a function of oxygen concentration for Rb_xWO_y with $x = 0.19$, 0.23, and 0.27, and$2.80 \leq x \leq 3.07$. Three regions corresponding to $T_c < 2$ K (superconductivity suppressed region), $T_c \sim 3$ K (superconductivity uniform region) and $T_c > 3$ K (superconductivity enhanced region) were identified in T_c–y phase diagram for $Rb_{0.19}WO_y$ and $Rb_{0.23}WO_y$. No superconductivity enhanced region was observed for $Rb_{0.27}WO_y$. For $Rb_{0.19}WO_y$ and $Rb_{0.23}WO_y$ samples, T_c is around 3 K in the low oxygen concentration regime and is then suppressed below 2 K as oxygen concentration y increases. When the oxygen concentration y increases further, T_c goes above 3 K and even reaches up to 5 K. The superconductivity suppressed region is in $2.85 < y < 2.95$ for

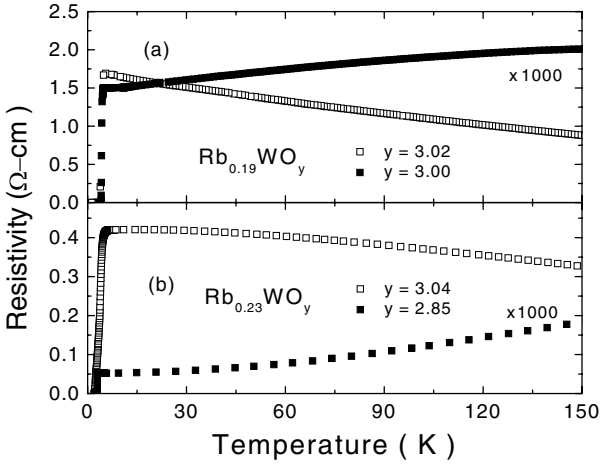

Fig. 5. (a) Resistivity as a function of temperature for $Rb_{0.19}WO_y$ with $y = 3.00$ and 3.02. (b) Resistivity as a function of temperature for $Rb_{0.23}WO_y$ with $y = 2.85$ and 3.04.

$Rb_{0.19}WO_y$ and $2.95 \leq y \leq 3.00$ for $Rb_{0.23}WO_y$, respectively. The reentrance and enhancement of T_c at $y \sim 2.95$ and 3.00 for $Rb_{0.19}WO_y$ and $Rb_{0.23}WO_y$, respectively, as well as the suppression of T_c at $y \sim 3.00$ for $Rb_{0.27}WO_y$, strongly suggest that there is no correlation between superconductivity and oxygen-concentration-dependent metal–nonmetal transition observed in Rb_xWO_y with $y \sim 3.00$ [16]. In addition, it can be deduced from Fig. 6 that the anomalous $T_c(x)$ dependence for Rb_xWO_3 with $0.23 \leq x \leq 0.28$ reported earlier is likely associated with a small deviation of the oxygen concentration from 3.00.

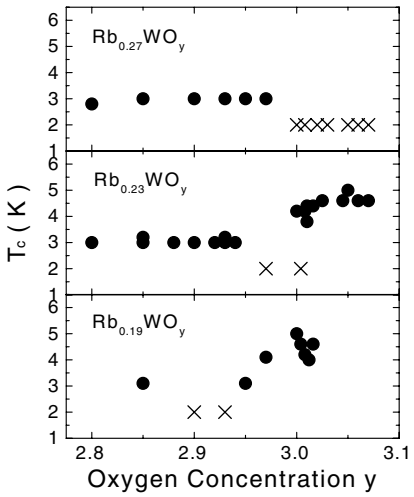

Fig. 6. Oxygen concentration dependence of the T_c for Rb_xWO_y with $x = 0.19$, 0.23, and 0.27, and $2.80 \leq y \leq 3.07$. The × marked at 2 K means that superconductivity was not observed down to 2 K.

Finally, let us offer possible scenarios account for the $T_c(y)$ dependence as well as the superconducting properties of Rb_xWO_y. The lower superconducting transition temperature accompanied by the sharper superconducting transition width is consistently observed in Rb_xWO_y with lower oxygen concentrations regardless of the value of the rubidium concentration x, suggesting that superconductivity observed in these compounds might have two different origins. The electron-phonon interaction weakened by the screening effect of the carriers is certainly not able to explain the observed phenomenon. The ordering of the rubidium atoms induced by the oxygen vacancy site in the WO_6 matrix may play an important role in the superconductivity present in the low oxygen concentration regime. While in the excess oxygen concentration regime, we speculate that the ordering of the rubidium atoms would be greatly influenced by the oxygen atoms sliding into the tunnels. This in turn would induce a local structure distortion and give rise to distinct superconducting properties. X-ray absorption and photoemission studies are undergoing to probe the possible local structure distortion and associated electronic excitation in Rb_xWO_y.

4. CONCLUSION

In summary, we report the effect of oxygen concentration on superconducting properties of rubidium tungsten bronzes Rb_xWO_y with $x = 0.19$, 0.23, and 0.27 and $2.80 \leq y \leq 3.07$. Three regions corresponding to $T_c < 2\,K$ (superconductivity suppressed region), $T_c \sim 3\,K$ (superconductivity uniform region) and $T_c > 3\,K$ (superconductivity enhanced region) were identified in T_c–y phase diagram for $Rb_{0.19}WO_y$ and $Rb_{0.23}WO_y$. No superconductivity enhanced region was observed for $Rb_{0.27}WO_y$. The local ordering of the intercalated rubidium atoms might be responsible for the intriguing T_c–y phase diagram of Rb_xWO_y.

ACKNOWLEDGEMENT

This work was financially supported by the ROC National science Council under grant No. NSC90-2112-M-032-020.

REFERENCES

1. C. J. Raub, A. R. Sweedler, M. A. Jensen, S. Broadston, and B.T. Matthias, *Phys. Rev. Lett*. **13,** 746 (1964).
2. G. Hollinger, P. Pertosa, J. P. Doumere, F. J. Himpsel, and B. Reihl, *Phys. Rev. B* **32,** 1987 (1985).
3. M. M. Dobson, J. L. Huchison, R. J. D. Tilley, and K. A. Watts, *J. Solid State Chem.* **71,** 47 (1987).
4. R. K. Stanley, R. C. Morris, and W. G. Moulton, *Phys. Rev. B* **20,** 1903 (1979).
5. S. T. Triantafyllou, P. C. Christidis, and Ch. B. Lioutas, *J. Solid State Chem.* **134,** 344 (1997).
6. H. R. Shanks, *Solid State Commun.* **15,** 752 (1974).
7. R. Salchow, R. Liebmann, and J. Appel, *J. Phys. Chem. Solids.* **44**, 245 (1983).
8. A. Narath and D. C. Barham, *Phys. Rev.* **176,** 479 (1968).
9. N. Tsuda, K. Nasu, A. Fujimori, and K. Siratori, *Electronic Conduction in Oxides,* p. 198 (Springer, Berlin, Heidelberg, 2000).
10. H. Hochst, R. D. Bringans, and H. R. Shanks, *Phys. Rev. B* **26,** 1702 (1982).
11. R. Brusetti, P. Haen, and J. Marcus, *Phys. Rev. B* **65,** 144528 (2002).
12. M. R. Skokan, W. G. Moulton, and R. C. Morris, *Phys. Rev. B* **20,** 3670 (1979).
13. L. H. Cadwell, R. C. Morris, and W. G. Moulton, *Phys. Rev. B* **23,** 2219 (1979).
14. R. Brusetti, P. Bordet, and J. Marcus, *J. Solid State Chem.* **172,** 148 (2003).
15. M. Sato, B. H. Grier, G. Shirane, and H. Fujishita, *Phys. Rev. B* **25,** 501 (1982).
16. L. C. Ting, H. H. Hsieh, C. T. Huang, C. B. Wang, D. C. Ling, K. J. Huang, S. J. Chang, H. H. Kang, F. Z. Chien, and P. H. Hor, *J. Superconductivity: Incorporating Novel Magnetism,* **15,** 675 (2002).
17. A. Magneli, *Acta Chem. Scand.* **7,** 315 (1953).